ACS OMEGA

http://pubs.acs.org/journal/acsodf

Article

Carbazoles in Oils, and Their Application in Identifying Oil Filling Pathways in Eocene Syn-Rift Fault Blocks in the Dongpu Depression, Bohai Bay Basin, East China

Youjun Tang,[#] Ruilin Wang, Donglin Zhang, Xiaoqiang Liu, Hongbo Li, Tianwu Xu, Yunxian Zhang, Chengfu Zhang, Yahao Huang, and Ting Wang*

Cite This: *ACS Omega* 2022, 7, 8103−8114

Read Online

ACCESS | Metrics & More | Article Recommendations

ABSTRACT: Carbazoles and dimethyl carbazoles (DMCs) are important nitrogen heterocyclic aromatic compounds in oils and sedimentary rock extracts. Based on both migration fractionation effects and differences in the thermal stability of their isomers, carbazoles can be used to trace oil migration orientations and filling pathways. Molecular biomarker compositions indicate that all oils and oil-bearing sand extracts in the Eocene fault-blocked reservoirs of the Huzhuangji area (Western Slope Belt) of the Dongpu Depression (Bohai Bay Basin, East China) belong to a single oil population. In this study, four geochemical indicators relating to carbazoles, namely (a) 1,8-/2,7-dimethyl carbazoles (1,8-/2,7-DMC); (b) 1,8-/2,5-dimethyl carbazoles (1,8-/2,5-DMC); (c) 1,8-/N-exposed dimethyl carbazoles (1,8-/N-exposed DMC); and (d) G1 N-shielded %, were applied to trace oil migration orientations and filling pathways. The results show that these parameter values gradually increase toward the Hu-5 fault block at the structural high. The measured values from the subsurface are consistent with the results calculated from the molecular adsorption modeling. Therefore, it is concluded that the relative parameters of dimethyl carbazoles are practical molecular indicators for tracing oil migration orientations and filling pathways in syn-rift fault-blocked reservoirs.

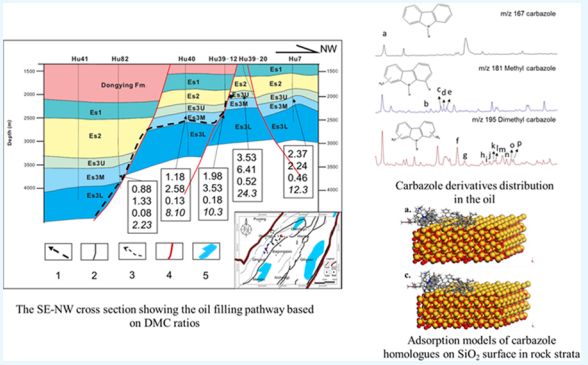

The SE-NW cross section showing the oil filling pathway based on DMC ratios

Adsorption models of carbazole homologues on SiO_2 surface in rock strata

1. INTRODUCTION

Complex fault-blocked sandstone reservoirs account for a considerable proportion of oil and gas production in China.[1] Sandstone reservoirs, especially fault-blocked or tight sandstone,[2−4] generally experience complex diagenetic histories that have progressively changed the reservoir quality.[2,3,5−7] Reservoir quality is controlled by multiple factors, such as detrital composition, depositional environment, sedimentary facies, burial temperature, pressure, and chemical composition of the pore water.[2,8] All of these factors bring challenge to the reconstruction of oil migration directions and pathways in such type of fault-blocked petroleum systems. A better understanding of the hydrocarbon migration process is crucial to determine potential source kitchens, predict "satellite reservoirs", and furthermore, to make exploration and exploitation plans.[9] Since seismic or other remote-sensing approaches cannot offer explicit secondary oil migration information, some molecular markers, such as carbazoles, their alkylated homologues, and benzocarbazoles, have been used as effective tracing indicators of oil migration and filling pathways.[10−12] With the development of gas chromatography (GC) and gas chromatography−mass spectrometry (GC−MS) since the 1970s, C_{1-10} alkylpyridines and C_{1-9} alkylquinolines in the basic fraction, along with carbazoles, C_{1-4} alkylcarbazoles, benzocarbazoles, and C_{1-4} alkylbenzocarbazoles in the neutral fraction, were discovered in the nitrogen-rich Boscan crude oil.[13−16]

In carbazoles, a hydrogen bond can be generated between the N−H functional group and the atoms with higher electronegativity. This course can lead to molecular adsorption and fractionation of carbazole isomers during oil migration.[10,11,17,18] Therefore, carbazoles can be used to determine the pathway and distances of oil migration. Li et al. discussed the interactions of aromatic nitrogen heterocycles with surface or formation water via hydrogen bonding, and ionic or hydrogen bonding.[11,18] Li et al. reported the enrichment of alkylcarbazoles relative to alkylbenzocarbazoles and the preferential enrichment of nitrogen-shielded isomers to nitrogen-exposed isomers in crude oils.[11] Larter et al. proposed that the benzocarbazole isomers are

Received: January 1, 2022
Accepted: February 14, 2022
Published: February 23, 2022

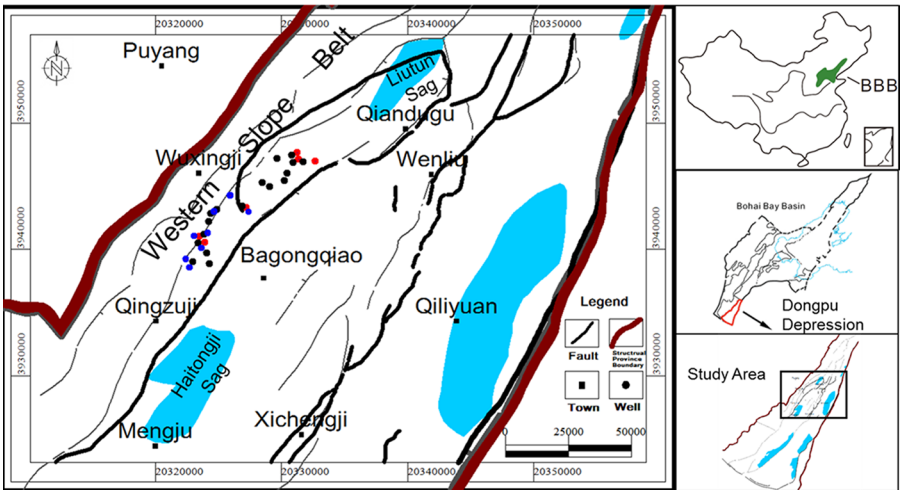

Figure 1. Map showing the location of the examined crude oil samples relative to major geological features and hydrocarbon plays in the study area. Red dots denote upper Es3 wells, black denote middle Es3, and blue denote lower Es3. BBB is short for Bohai Bay Basin.

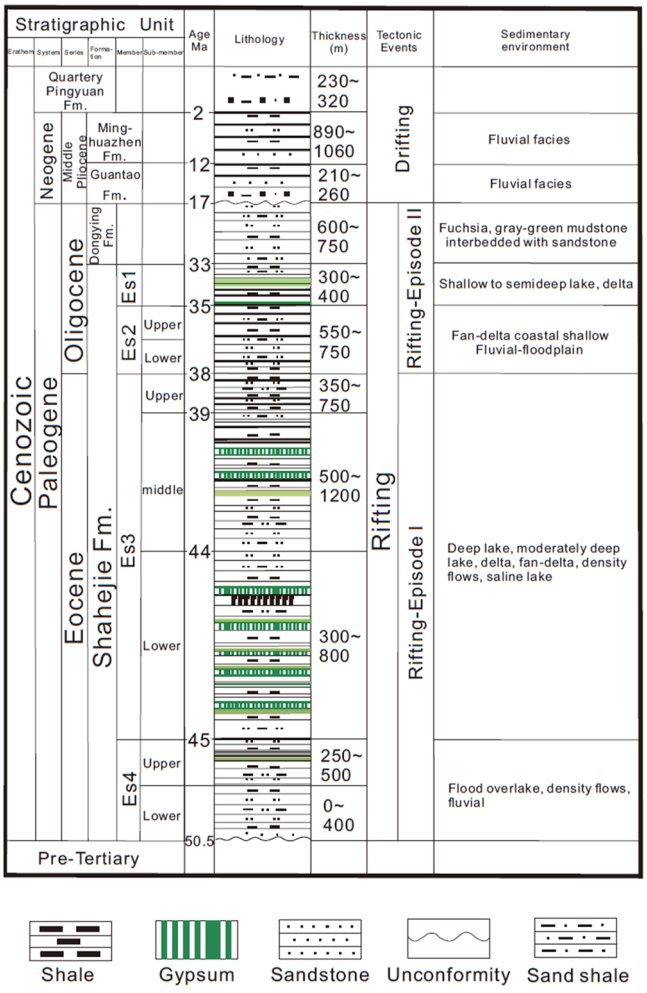

Figure 2. Generalized stratigraphy and tectonic events of the Huzhuangji area, Dongpu Depression (after ref 39). Reprinted (adapted or reprinted in part) with permission from [Zhang, D.L.; Tang, Y.J.; Li, H.B.; Xu, T.W.; Zhang, Y.X.; Zhang, C.F.; Huang, Y.H.; Wang, T. Methyltrimethyltridecylchromans in Mature Oils from Saline Lacustrine Settings in the Dongpu Depression, Bohai Bay Basin, East China. ACS omega. 2021, 6(27): 17400-17412. DOI: 10.1021/ACSOMEGA.1C01688]. Copyright [2021] [ACS Publications].

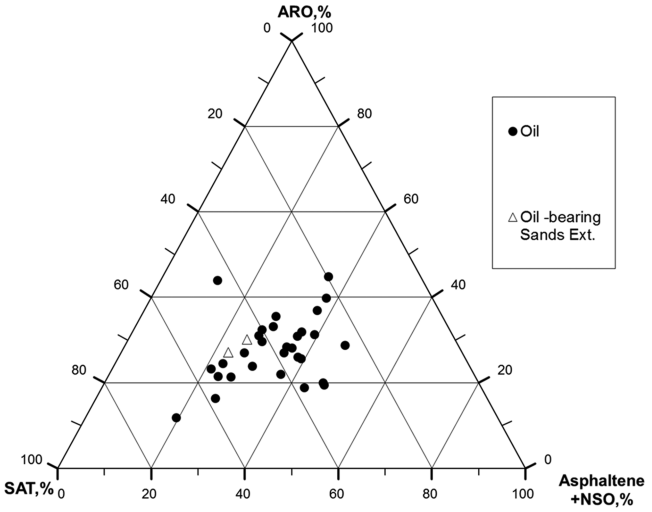

Figure 3. Ternary diagram showing the proportion of saturated hydrocarbon (SAT), aromatic hydrocarbon (ARO), asphaltene, and NSO compounds (NSO) in Eocene oils from the Huzhuangji area, Dongpu Depression.

absorbed by clay minerals or carbonates, and the BC ratio (benzo [c]/[c] + [a] carbazole) could be used as an indicator of migration distances.[10] Because of their high polarity, organic nitrogen compounds exhibit a strong absorption/adsorption behavior when in contact with solid organic/mineral phases and are more water soluble than hydrocarbons. These effects vary as result of the molecular structure of individual organic nitrogen compounds, and hence, their relative abundance should gradually change during oil migration.[12,19−22]

The proposed migration parameters should be used with caution as more recent studies have shown that the distributions of organic nitrogen compounds can also be affected by other factors such as maturity, biodegradation, or depositional environment.[12,22−28] However, there are still a number of studies that showed that methylcarbazoles and benzocarbazoles could be useful for studying migration distances as long as the samples are kept at approximately the same maturity level.[29−32]

The petroleum system of the Western Slope Belt of the Dongpu Depression is characterized by multisource kitchens, multisets of reservoir−cap rock combination, various trap types,

https://doi.org/10.1021/acsomega.2c00003
ACS Omega 2022, 7, 8103−8114

Table 1. Bulk Properties of Oils from the Dongpu Depression, Bohai Bay Basin, East China[a]

well	code	formation	depth (m)	density (g/cm^3)	% SAT	% ARO	% NSO + ASP
Hu12−17	A-1	Upper Es3	2168.5−2202.4	0.91	46.5	23.9	29.7
Hu5−227	A-2	Upper Es3	2331.3−2557.1	0.89	46.6	27.1	26.3
Hu5−39	A-3	Upper Es3	2040.3−2108.8	0.90	32.9	30.5	36.6
Hu21−4	A-4	Upper Es3	1904.4−2181.4	0.92	34.6	28.5	36.9
Hu10−10	A-5	Upper Es3	1776.2−1834.0	0.93	35.7	26.0	38.3
Hu39−20	A-6	Upper Es3	1748.5−1880.1	0.87	37.4	33.2	29.4
Hu2−3	B-1	Middle Es3	2692.6−2766.8	0.88	38.4	26.5	35.1
Hu2−4	B-2	Middle Es3	2029.6−2120.1	0.86	38.4	28.5	33.1
Hu39−21	B-3	Middle Es3	1781.4−1872.3	0.84	33.6	28.5	37.9
Hu7−139	B-4	Middle Es3	1754.8−1798.0	0.86	44.4	30.2	25.4
Hu7−115	B-5	Middle Es3	1886.6−1888.1	0.86	37.4	26.5	36.1
Hu7−34	B-6	Middle Es3	1730.6−1771.0	0.88	39.0	28.5	32.5
Hu12−166	B-7	Middle Es3	2168.5−2202.4	0.86	46.5	23.9	29.7
Hu52−3	B-8	Middle Es3	2561.8−2594.3	0.86	22.7	39.8	37.4
Hu5−130	B-9	Middle Es3	2051.8−2203.0	0.86	34.1	26.5	39.4
Hu5−11	B-10	Middle Es3	2160.6−2199.1	0.86	35.2	30.5	34.3
Hu5−202	B-11	Middle Es3	2160.9−2163.0	0.84	33.8	30.5	35.7
Hu12−173	B-12	Middle Es3	2168.5−2202.4	0.86	33.6	27.5	38.9
Hu5−125	B-13	Middle Es3	2031.0−3001.5	0.85	39.4	29.5	31.1
Hu5−247	B-14	Middle Es3	2331.3−2557.1	0.86	46.6	27.1	26.3
Hu7−19	C-1	Lower Es3	2000.6−2469.4	0.86	41.3	30.7	28.0
Hu7−137	C-2	Lower Es3	1953.1−2091.0	0.85	29.3	26.5	44.2
Hu7−95	C-3	Lower Es3	2175.8−2219.0	0.85	35.0	27.5	37.5
Hu62−5	C-4	Lower Es3	2655.3−2797.5	0.87	35.6	35.6	28.8
Hu12−161	C-5	Lower Es3	2231.6−2387.0	0.85	31.8	27.5	40.7
Hu12−34	C-6	Lower Es3	2477.2−2532.0	0.85	34.6	29.5	35.9
Hu10−18	C-7	Lower Es3	2225.3−2375.9	0.85	31.7	28.5	39.8
Hu39−12	C-8	Lower Es3	2637.8−3250.0	0.85	37.9	18.9	43.2
Hu82	oil sand	Lower Es3	4215.9	NA	43.5	22.6	33.9
Hu40	oil sand	Lower Es3	3890.4	NA	38.2	36.0	25.8

[a]Code: well codes; SAT: saturated hydrocarbon; ARO: aromatic hydrocarbon; NSO: resins; ASP: asphaltene.

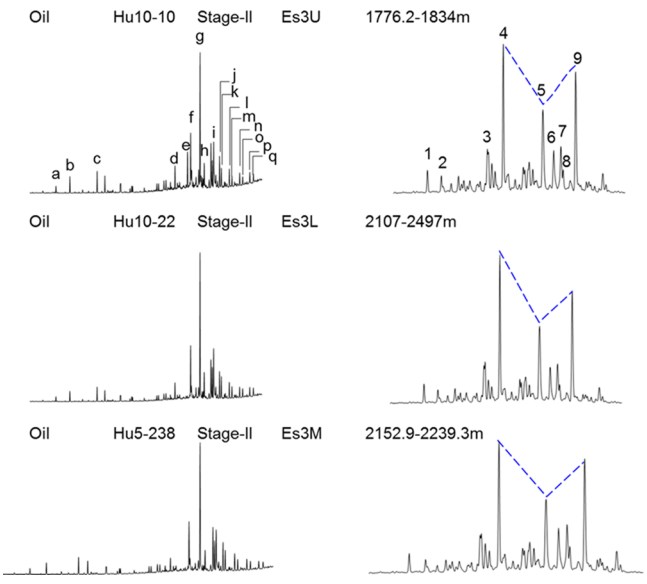

Figure 4. Mass chromatograms showing the distribution of terpanes (m/z 191) and steranes (m/z 217) in oils from the Huzhuangji area, Dongpu Depression, Bohai Bay Basin. Peak assignments for terpanes and steranes are displayed in Table 3.

and multistage hydrocarbon accumulation.[32] The source of the oil and gas produced from the Western Slope Belt is still in dispute.[33] Some studies concluded that the oil was derived from the middle submember of the third member of the Eocene Shahejie Formation to the lower submember of the third member of the Eocene Shahejie Formation (Es3M−Es3L) in the dark mudrock of the Liutun and Haitongji Sags.[34−37] Some authors commented that the oil was sourced from the Es3M mudstone of the Haitongji Sag and partially from the Liutun Sag.[38,39] Tang held a different opinion that the oil was mainly sourced from the Haitongji Sag, while mixed with a minor contribution *in situ* from the Es1−Es3−Es4 oil shale of the Western Slope Belt.[40] In brief, most of the previous studies agreed that the major source beds for most oil discoveries found in the Shahejie Formation of the Western Slope Belt would be the organic-rich dark mudstones in the Haitongji Sag.[39,41−43] In addition, most of the oils previously reported in the study area share pretty similar physical properties and bulk geochemical characteristics. However, the extent of variation within the organic nitrogen compounds during migration, especially in such complicated faulted blocks like that in this study, is still poorly understood. Therefore, this study reports the application of these indicators in a typical lacustrine syn-rift fault-blocked sandstone reservoir in the Huzhuangji area (Western Slope Belt) of the Dongpu Depression of the Bohai Bay Basin (BBB), East China.

2. GEOLOGICAL SETTINGS

The NNE-trending Dongpu Depression in the southwestern part of the Bohai Bay Basin is a typical rift basin formed after the strong fault depression during the late Mesozoic (Figure 1). It is

https://doi.org/10.1021/acsomega.2c00003
ACS Omega 2022, 7, 8103−8114

Table 2. Selected Molecular Geochemical Parameters for Oils from the Dongpu Depression, Bohai Bay Basin, East China[a]

						steranes $\alpha\alpha\alpha$ R (%)							
sample	code	$C_{29}H/C_{30}H$	$G/C_{30}H$	$C_{35}H/C_{34}H$	DiaSter27/Ster27	C_{27}	C_{28}	C_{29}	MPI-1	1,8-/2,7-DMC	1,8-/2,5-DMC	1,8-/N-exposed DMC	G1 N-shielded %
Hu12−17	A-1	0.36	0.47	0.97	0.24	0.37	0.30	0.33	0.66	NA	3.73	0.83	19.88
Hu5−227	A-2	0.38	0.34	0.87	0.38	0.37	0.29	0.34	0.56	NA	1.20	0.33	9.90
Hu5−39	A-3	0.38	0.32	0.88	0.41	0.37	0.30	0.33	0.55	NA	0.71	0.17	6.70
Hu21−4	A-4	0.38	0.33	0.86	0.43	0.38	0.30	0.33	0.61	NA	1.31	0.30	8.35
Hu10−10	A-5	0.42	0.53	1.03	0.22	0.37	0.30	0.33	0.64	NA	3.70	0.37	16.87
Hu39-20	A-6	0.35	0.34	0.76	0.23	0.36	0.30	0.35	0.58	NA	6.41	0.54	24.30
Hu2−3	B-1	0.38	0.30	0.86	0.40	0.37	0.29	0.34	0.54	1.02	1.85	0.25	7.49
Hu2−4	B-2	0.38	0.33	0.87	0.39	0.37	0.30	0.33	0.55	1.74	1.20	0.38	10.00
Hu39−21	B-3	0.41	0.34	0.44	0.36	0.38	0.29	0.33	0.54	2.65	2.62	0.54	15.11
Hu7−139	B-4	0.35	0.41	0.92	0.31	0.34	0.30	0.36	0.59	2.37	2.24	0.46	12.30
Hu7−115	B-5	0.33	0.39	0.88	0.31	0.33	0.29	0.36	0.62	1.52	1.82	0.37	10.50
Hu7−34	B-6	0.36	0.41	0.93	0.33	0.34	0.30	0.36	0.66	2.00	1.60	0.37	10.11
Hu12−166	B-7	0.36	0.47	0.49	0.26	0.37	0.31	0.33	0.64	3.03	1.89	0.57	13.30
Hu52−3	B-8	0.38	0.55	0.84	0.18	0.38	0.29	0.33	0.52	1.81	1.24	0.38	9.71
Hu5−130	B-9	0.38	0.30	0.87	0.41	0.37	0.29	0.34	0.56	1.98	1.56	0.43	12.20
Hu5−11	B-10	0.38	0.33	0.86	0.39	0.37	0.30	0.33	0.57	2.50	1.54	0.48	13.30
Hu5−202	B-11	0.27	0.31	0.88	0.42	0.37	0.29	0.34	0.56	2.60	1.61	0.49	13.20
Hu12−173	B-12	0.38	0.48	0.46	0.26	0.37	0.30	0.33	0.53	2.05	1.68	0.41	10.86
Hu5−125	B-13	0.38	0.30	0.87	0.41	0.37	0.29	0.34	0.56	1.09	0.92	0.30	9.11
Hu5−247	B-14	0.38	0.35	0.79	0.16	0.37	0.29	0.34	0.52	2.01	2.80	0.51	17.90
Hu12−158	B-15	0.40	0.49	0.45	0.22	0.37	0.30	0.33	0.56	11.51	7.75	1.15	32.20
Hu5−238	B-16	0.37	0.40	0.82	0.19	0.35	0.30	0.35	0.57	2.68	5.26	0.80	22.00
Hu12−59	B-17	0.36	0.48	0.88	0.26	0.37	0.31	0.33	0.56	1.89	1.79	0.41	10.40
Hu7−19	C-1	0.36	0.44	0.91	0.33	0.34	0.30	0.36	0.54	1.66	1.78	0.35	9.86
Hu7−137	C-2	0.35	0.41	0.92	0.31	0.34	0.30	0.36	0.59	1.78	1.55	0.34	9.52
Hu7−95	C-3	0.33	0.39	0.89	0.33	0.32	0.29	0.36	0.62	2.13	1.87	0.43	11.51
Hu62−5	C-4	0.37	0.55	0.81	0.16	0.38	0.29	0.33	0.65	1.41	1.11	0.30	8.95
Hu12−161	C-5	0.40	0.49	0.45	0.22	0.37	0.30	0.33	0.64	1.32	1.29	0.33	9.00
Hu12−34	C-6	0.38	0.49	0.45	0.26	0.37	0.30	0.33	0.53	1.30	1.18	0.30	8.70
Hu10−18	C-7	0.42	0.55	1.05	0.20	0.38	0.29	0.33	0.56	1.43	1.37	0.33	9.77
Hu39−12	C-8	0.41	0.34	0.44	0.36	0.38	0.29	0.33	0.58	1.98	3.53	0.18	10.30
Hu82	oil sand	0.50	0.30	0.46	0.42	0.34	0.29	0.37	0.56	0.88	1.33	0.08	2.23
Hu40	oil sand	0.57	0.25	0.88	0.46	0.37	0.29	0.34	0.54	1.18	2.58	0.13	8.10

[a] $C_{29}H/C_{30}H$: C_{29} 17α hopane/C_{30} 17α hopane; $G/C_{30}H$: gammacerane/C_{30} 17α hopane; $C_{35}H/C_{34}H$: C_{35} 17α homohopane/C_{34} 17α homohopane; DiaSter27/Ster27: [C_{27} 13β(H),17α(H)-diacholestane (20S + 20R)]/[C_{27} 14α(H),17α(H)- + 14β(H),17β(H)-cholestane (20S + 20R)]; C_{27}%, C_{28}%, C_{29}% = C_{27}, C_{28}, C_{29} [14α(H),17α(H)- + 14β (H),17β (H)-cholestane (20S + 20R)]; MPI-1: methyl phenanthrane index-1 = 1.5 × (3-MP + 2-MP)/(P + 9-MP + 1-MP); 1,8-/2,7-DMC: 1,8-/2,7-dimethyl carbazole; 1,8-/2,5-DMC: 1,8-/2,5-dimethyl carbazole; 1,8-/N-exposed DMC: 1,8-dimethyl carbazole/(2,6- + 2,7- + 2,4- + 2,5- + 2,3- + 3,4-dimethyl carbazole); G1 N-shielded %: 1,8-dimethyl carbazole/(1,8- + 1,3- + 1,6- + 1,7- + 1,4- + 4-ethyl dimethyl carbazole + 1,5- + 3-ethyl dimethyl carbazole + 2,6- + 2,7- + 1,2- + 2,4- + 2,5- + 2,3- + 3,4-dimethyl carbazole)*100%.

https://doi.org/10.1021/acsomega.2c00003
ACS Omega 2022, 7, 8103−8114

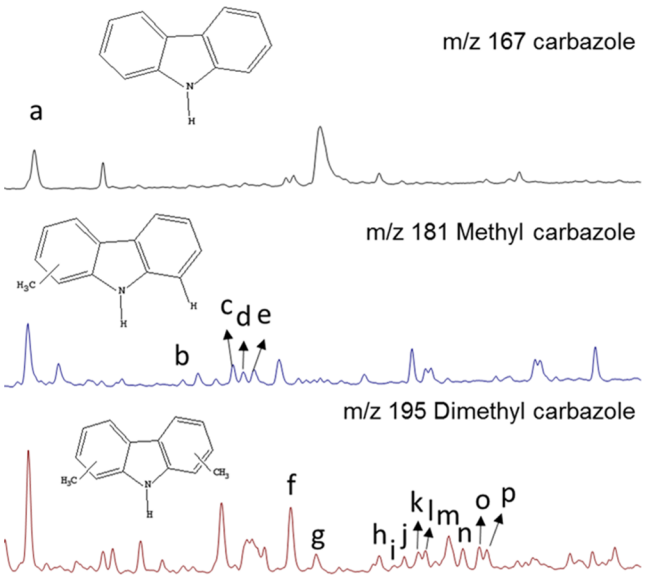

Figure 5. Chromatograms (m/z 167, 181, and 195) displaying the distribution of carbazole derivatives in the Hu39-12 oil, produced from the lower Es3 formation. The identifications of (a−p) are given in Table 4.

overlying the Neihuang Uplift in the west and bounded by the Lanxiao Fault and Luxi Uplift in the east, Lankao Uplift in the south, and Xinxiang Depression in the north (Figure 2).[44] The Dongpu Depression developed on the Ordovician−Cambrian and Carboniferous−Permian basements, which is overlain by Cenozoic sediments, including the Paleogene Shahejie (Es), Dongying (Ed), and Neogene Guantao (Ng) formations (Figure 2).[45] During the Cenozoic, the Dongpu Depression generally underwent two tectonic stages, Paleogene rifting and Neogene drifting, accumulating extremely thick sediments. The Cenozoic sediments have a maximum thickness of more than 9000 m, of which the Paleogene sediments are over 6000 m thick. The Shahejie Formation (Es) is divided into four members (Es1−Es4). Es3 and Es4 are further divided into three ($Es3^1$−$Es3^3$) and two ($Es4^1$ and $Es4^2$) submembers. The Es4 member and middle−lower Es3 submembers ($Es3^2$−$Es3^3$) were deposited in a humid climate and consist of extensive and deep lacustrine facies. The $Es3^1$ submember denotes arid fluvial facies, and the Es1−Es2 members represent shallow lacustrine facies deposited in a humid climate.[38,46−48] Es3 was the main stage for the formation of hydrocarbon source rocks, salts, and favorable reservoirs, during which time the saline lacustrine sediments were well developed.

The study area is located in the middle of the Western Slope Belt of the Dongpu Depression, covering from the south of Huzhuangji to Well Hu-19 in the north, reaching the Wuxingji Fault in the west, and the eastern side of Changyuan Fault in the East (Figure 1). The Wuxingji Fault, Shijiaji Fault, and Changyuan Fault in the Western Slope Belt are controlled by three N-NE trending fault systems, which cut the ramp belt into three stepped belts, namely, step I, II, and III (Figure 2). The footwall of the Changyuan Fault is defined as step I. The footwall between the Changyuan Fault and the Shijiaji Fault is defined as step II, and that between the Shijiaji Fault and the Wuxingji Fault as step III.[49,50] Each step has different fault development characteristics and structural patterns (Figure 2).

3. RESULTS AND DISCUSSION

3.1. Bulk Properties of Oils. The general properties of oils from the Huzhuangji area of the Dongpu Depression are shown in Table 1 and Figure 3. These oils are characterized by medium density (0.81−0.93 g/cm^3). The relative abundance of saturated hydrocarbons is low (22.7−46.6%, with an average of 35.9%). The proportions of asphaltenes (ASP) and resins (NSOs) are high, within a range of 25.4−43.5%. Crude oils exhibit slight differences in bulk parameters that are consistent with the type of fluid, in which the majority of the samples are classified as medium to black oil. The crude oil bulk characteristic is a useful descriptive source of data, with some inherent limits. The relatively medium density of the oil samples is reasonable to be found in thermogenic hydrocarbon expelled from mature source

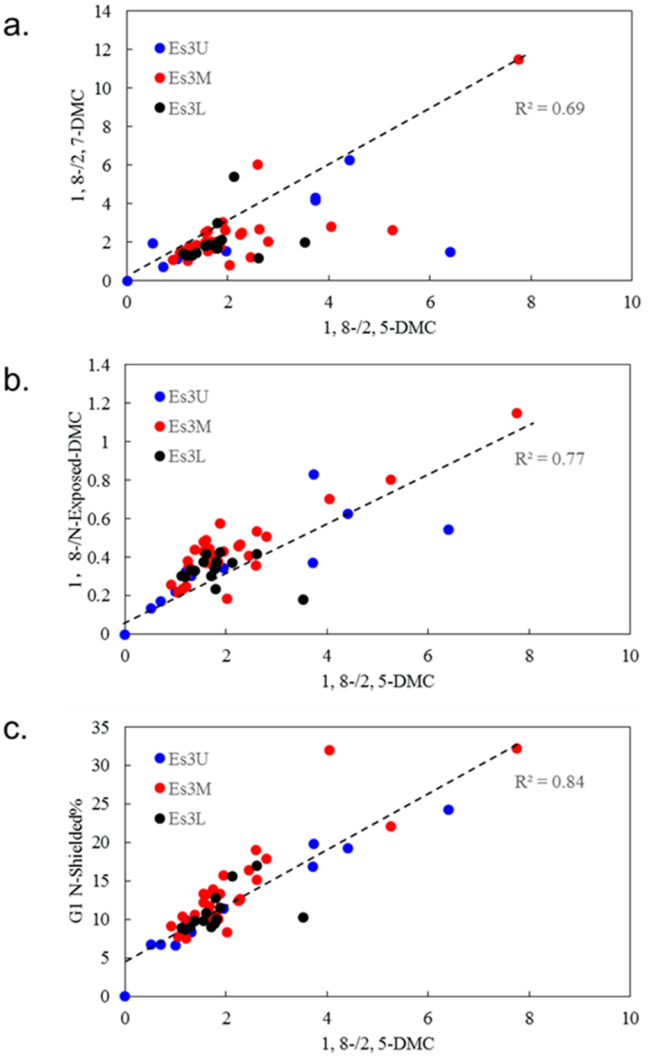

Figure 6. Relationship between different carbazole ratios of the examined oils from the Western Slope Area of Dongpu Depression: (a) 1,8-/2,7-DMC vs 1,8-/2,5-DMC; (b) 1,8-/N-exposed DMC vs 1,8-/2,5-DMC; and (c) G1 N-shielded % vs 1,8-/2,5-DMC. Es3U denotes oils produced from the upper member of the Eocene Shahejie Formation. Es3M: the middle member of the Eocene Shahejie Formation; Es3L: the lower member of the Eocene Shahejie Formation. DMC: dimethyl carbazole. 1,8-/N-exposed DMC: 1,8-DMC/(2,6- + 2,7- + 2,4- + 2,5- + 2,3- + 3,4-DMC). G1 N-shielded %: 1,8-DMC/(1,8- + 1,3- + 1,6- + 1,7- + 1,4- + 4-ethyl DMC + 1,5- + 3-ethyl DMC + 2,6- + 2,7- + 1,2- + 2,4- + 2,5- + 2,3- + 3,4-DMC)*100%.

https://doi.org/10.1021/acsomega.2c00003
ACS Omega 2022, 7, 8103−8114

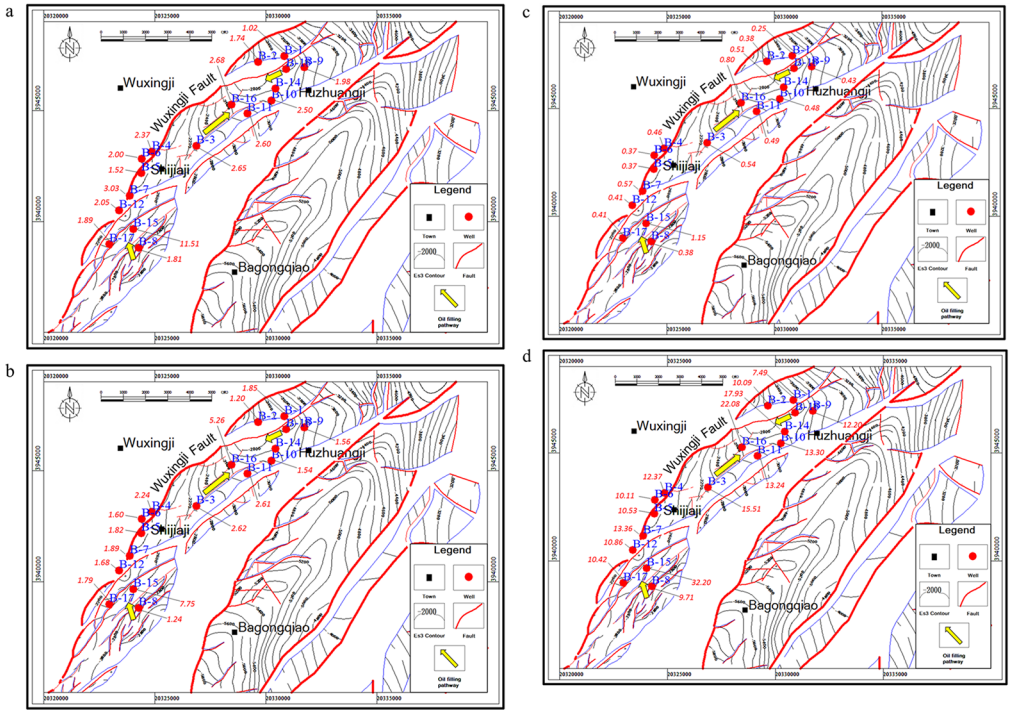

Figure 7. Carbazole isomer ratios on the middle Es3 contour map tracing oil filling pathways in the Eocene lacustrine clastic reservoirs, Huzhuangji Area, Dongpu Depression. (a) 1,8-/2,7-Dimethylcarbazole; (b) 1,8-/2,5-dimethyl carbazole; and (c) 1,8-/nitrogen-exposed dimethyl carbazole. (d) Relative abundance of G1 nitrogen-shielded dimethyl carbazole.

Table 3. Peak Assignments for Terpanes and Steranes Labeled in Figure 3

peak#	compound
a	C_{20} tricyclic terpane (Cheilanthane)
b	C_{21} tricyclic terpane (Cheilanthane)
c	C_{23} tricyclic terpane (Cheilanthane)
d	C_{27} 18α(H)-22,29,30-trisnorneohopane (Ts)
e	C_{27} 17α(H)-22,29,30-trisnorhopane (Tm)
f	C_{29} 17α(H),21β(H)-30-norhopane (H29)
g	C_{30} 17α(H),21β(H)-hopane
h	C_{30} 17β (H),21α (H)-moretane
i	gammacerane
j, k	C_{32} 17α(H),21β(H)-bishomohopane (22S & 22R)
l, m	C_{33} 17α(H),21β(H)-trishomohopane (22S & 22R)
n, o	C_{34} 17α(H),21β(H)-tetrakishomohopane (22S & 22R)
p, q	C_{35} 17α(H),21β(H)-pentakishomohopane (22S & 22R)
1	13β(H),17α(H)-diacholestane (20S)
2	13β(H),17α(H)-diacholestane (20R)
3	14α(H),17α(H)-cholestane (20S)
4	14α(H),17α(H)-cholestane (20R)
5	24-methyl-14α(H),17α(H)-cholestane (20R)
6	24-ethyl-14α(H),17α(H)-cholestane (20S)
7	24-ethyl-14β(H),17β(H)-cholestane (20R)
8	24-ethyl-14β(H),17β(H)-cholestane (20S)
9	24-ethyl-14α(H),17α(H)-cholestane (20R)

rocks. Moreover, such enrichment in asphaltenes and NSOs has been reported in typical saline oils.[41,43,51] Considering that the salt-bearing strata are well-developed during the Eocene in the northern part of the Dongpu Depression, it is reasonable to find such typical saline oils in the study area.[39]

3.2. Oil-to-Oil Correlation. The distributions of steranes and terpanes have been widely used as correlation tools.[52] Genetic relationships between oil samples can be established by comparing the similarity of their fingerprints.[53,54] As shown in Figure 4, the m/z 191 and 217 mass chromatogram fingerprints of the step II crude oil from upper Es3 (1776.2−1834 m in Well Hu10−10) are consistent with those of the step II oil of middle Es3 (2107−2497 m in Well Hu10−22) and the step II oil of lower Es3 (2152.9−2239.3 m in Well Hu10−22). All of the three oils show a normal distribution pattern of regular tricyclic terpanes with C_{23} as the dominant component in the m/z 191 mass chromatogram, suggesting their OM sources were consistent, mainly lower aquatic organisms in saline lakes. The source beds would have a relatively low content of marly limestone (without C_{35} homohopane predominance). As shown in Table 2 and Figure 4, oil samples from the Huzhuangji area of the Dongpu Depression are relatively abundant in gammacerane with gammacerane/C_{30} hopane ratios of 0.25−0.55, averaging 0.40, and diasteranes with moderate C_{27} diasterane/C_{27} sterane (0.16−0.46) ratios averaging 0.40 and 0.31, respectively, which may imply clay-rich source rocks deposited in a stratified water column with variable amounts of higher plant inputs. In addition, the contents of C_{27} and C_{29} regular steranes are relatively high. The distributions of C_{27}, C_{28}, and C_{29} regular steranes show an asymmetric "V" shape in all graphs of the samples, which indicates a continental lacustrine characteristic of mixed organic materials with dominant aquatic organisms and variable higher plant inputs. These samples clearly belong to the same oil family.

3.3. Qualitative Analyses of Carbazole Series in Oils. By comparison with the relative retention times and retention indices on m/z 167, 181, and 195 mass chromatograms published by Li et al. and Larter et al.,[10−12] carbazoles, methylcarbazoles (MCs), and dimethyl carbazoles (DMCs) can be identified in oil samples from the Huzhuangji area (Western Slope Belt) of the Dongpu Depression on a DB-5MS

https://doi.org/10.1021/acsomega.2c00003
ACS Omega 2022, 7, 8103−8114

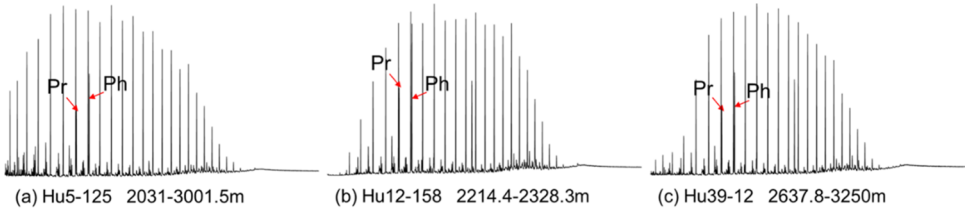

Figure 8. Typical gas chromatograms of the saturated fractions of crude oils in the study area (Western Slope Belt), Dongpu Depression.

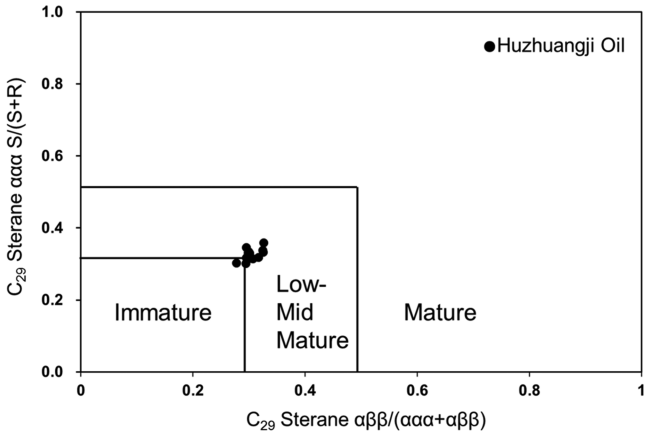

Figure 9. Crude oil sterane-based maturity parameter correlation diagram.

Table 4. Peak Assignments for Organic Nitrogen Compounds Labeled in Figure 4

peak#	compound
a	carbazole
b	1-methylcarbazole
c	3-methylcarbazole
d	2-methylcarbazole
e	4-methylcarbazole
f	1,8-dimethylcarbazole
g	1-ethylcarbazole
h	1,3-dimethylcarbazole
i	1,6-dimethylcarbazole
j	1,7-dimethylcarbazole
k	1,4-dimethylcarbazole + 4-ethylcarbazole
l	1,5-dimethylcarbazole + 3-ethylcarbazole
m	2,7-dimethylcarbazole
n	1,2-dimethylcarbazole
o	2,4-dimethylcarbazole

column by GC−MS (Figure 5). With coinjection of a known amount of phenantherene-D10 internal standard before the GC−MS analysis, the absolute concentrations of carbazole and its alkylated homologues can be determined.[10,12]

3.4. Optimized Carbazole Ratios for Tracing Oil Charging Pathways. In carbazoles, a hydrogen bond can be generated between the N−H functional group and the atoms with higher electronegativity, such as the oxygen atom in organic matter. This process may cause molecular adsorption and fractionation of carbazole isomers during oil migration.[10,12] Consequently, the fractionation effect of carbazole compounds can effectively indicate the direction of hydrocarbon migration.[10,14,55] Carbazole and its methyl and dimethyl isomers are detected in all of the 20 oil samples analyzed (Figure 5 and Table 2). Several pyrrolic parameters, like 1,8-/2,7-DMC and 1,8-/N-exposed DMC, have been reported to achieve good effects in the hydrocarbon migration pathway indication in several continental basins (Eastern China), such as the Songliao Basin (Wang et al.; He et al.) and the Bamianhe area of the Dongying Depression.[56−58] In this study, the pyrrolic compounds, including methyl and dimethyl isomers, are abundant in oils, with varying amounts in different samples. Therefore, four pyrrolic parameters, 1,8-/2,7-DMC, 1,8-/2,5-DMC, 1,8-/N-exposed DMC, and G1 N-shielded %, are selected to indicate the hydrocarbon migration to ensure the validity of the parameter analysis. In Figure 6, a good correlation is shown to be existing between any two of the four pyrrolic parameters regardless of the oil producing formation difference, which confirms the reliability of the optimized carbazole ratios to trace oil charging pathways in this study.

3.5. DMCs Tracing Oil Charging Pathways. It can be seen from Figure 7 that the pyrrolic parameters have an obvious varying trend. The overall hydrocarbon migration direction reflected by the varying trend of the four parameters (1,8-/2,7-DMC, 1,8-/2,5-DMC, 1,8-/N-exposed DMC, and G1 N-shielded %) is consistent. There are three major hydrocarbon migration directions. The values of the four parameters increase gradually from B-9 to B-16 in the northeastern part of the study area. The oil may come from the Liutun Sag in the NE.[41] In addition, the values of the four parameters are gradually increased from B-17 to B-16 via several wells along the Wuxingji Fault (Figure 7), which suggest the lateral migration along the Wuxingji Fault from SW to NE. Moreover, the trend is consistent with the structural dip of Es3M formation, which infers the hydrocarbon migrated along the Wuxingji Fault to the Hu-5 block (structural high) where B-16 is located. In the southwestern part of the study area, the four parameters showed low values in the B-8 oil (1.81, 1.24, 0.38, and 9.67, respectively) and relatively high values (11.51, 7.75, 1.15, and 32.2, respectively) in the B-15 oil, which are even higher than those in B-12, B-7, and other wells in the northward direction. This finding may indicate that the hydrocarbon migrated from B-8 to B-15 and was trapped there due to the possible fault sealing in B-15 (Table 3).

As mentioned above, the distributions of organic nitrogen compounds can also be affected by other factors such as maturity, biodegradation, or depositional environment; however, methylcarbazoles and benzocarbazoles could be effective oil migration tracers as long as the samples are kept at approximately the same maturity level.[22−27,29−32] The studied oils show no obvious biodegradation, as shown in Figure 8. The maturity parameters of saturates (Figure 9) or aromatics (MPI-1 values in Table 2) indicate an approximately consistent maturity range. Samples from the Eocene lacustrine clastic reservoirs in the Huzhuangji area of the Dongpu Depression belong to the same oil family and are nondegraded oils. Therefore, the variations in carbazole indicators in this study are mainly controlled by the oil-migration fractionation effect (Table 4).

https://doi.org/10.1021/acsomega.2c00003
ACS Omega 2022, 7, 8103−8114

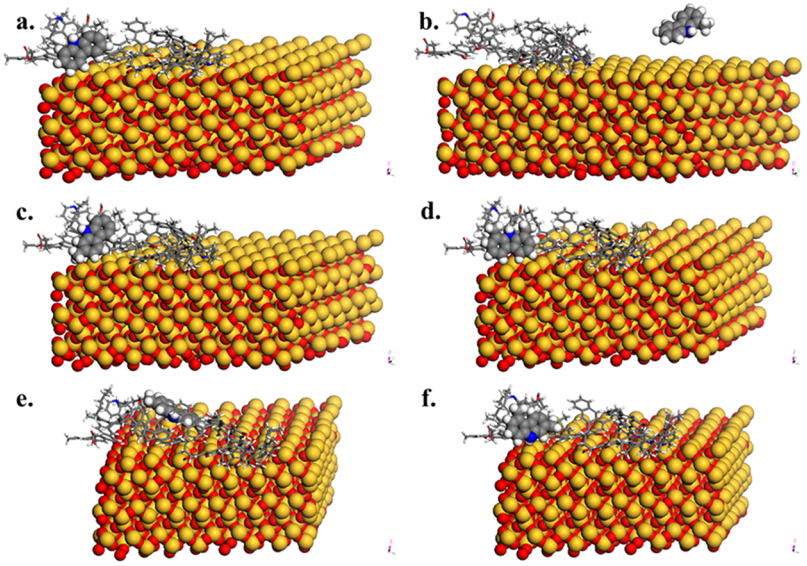

Figure 10. Adsorption models of carbazole homologues on the SiO_2 surface in the rock strata: (a) carbazole, (b) 1-MC, (c) 2-MC, (d) 1,8-DMC, (e) 2,7-DMC, and (f) 2,5-DMC. (after ref 59). Reprinted (Adapted or Reprinted in part) with permission from [Han, Q.Y.; Li, M.J.; Liu, X.Q.; Jiang, W.D.; Shi, S.B.; Tang, Y.J.; He, D.X. Fractionation of alkylated carbazoles in petroleum during subsurface migration: Evidence from molecular simulation and application in sandstone reservoirs. J. Pet. Sci. Eng. 2020, 191, 107308. DOI: 10.1016/j.petrol.2020.107308.]. Copyright [2020] [Elsevier].

Table 5. Interaction Energies and Dipole Moment of Carbazole, and MC and DMC Isomers[57]

		E ln (kcal/mol)
carbazole	μ (Debye)	SiO_2
CA	1.6692	−8.93
1-MC	1.9995	−6.08
2-MC	1.5116	−10.37
3-MC	1.7942	−8.77
4-MC	1.3244	−10.50
1,8-DMC	2.2870	−10.07
1,3-DMC	1.8846	−10.82
1,6-DMC	1.7942	−11.06
1,7-DMC	2.0470	−10.08
1,4-DMC	1.6586	−10.62
1,5-DMC	1.6534	−10.34
2,6-DMC	1.5207	−11.23
2,7-DMC	1.7613	−10.67
1,2-DMC	2.1554	−10.89
2,4-DMC	1.4841	−11.17
2,5-DMC	1.4732	−11.64
2,3-DMC	1.7347	−10.47
3,4-DMC	1.1471	−10.69

3.6. Molecular Simulation of Geochromatographic Fractionation of Carbazole Compounds on the Oil Filling Pathway. In this study, the polarity index, dipole moment of each carbazole compound, and molecular interaction between carbazoles and SiO_2 were simulated by molecular simulation to confirm the validity of the carbazole index as an effective migration index from the perspective of a chemical mechanism. A simulated SiO_2 adsorption model between carbazole homologues and rock strata proposed by our previous study is shown in Figure 10.[59] In previous studies, we carried out relevant molecular simulations and bond energy calculations (Table 5) to calculate the common indicators of carbazole compounds: (a) 1,8-/2,7-dimethyl carbazole = 0.94, (b) 1,8-/2,5-dimethyl carbazole = 0.86, (c) 1,8-/nitrogen-exposed dimethyl carbazole = 0.15, and (d) relative abundance of G1 nitrogen-shielded dimethyl carbazole = 0.06.[59] The values of the four mentioned indexes are all less than 1, indicating a decreasing trend of the DMCs abundance in the crude oils along the oil filling pathway but with different decreasing extents, which is positively correlated with the interaction energy between DMC and SiO_2. For example, 1,8-DMC has a weaker interaction energy with SiO_2 than 2,5-DMC (Table 5), indicating that 1,8-DMC would be more favorable to stay in the mobile oil phase than 2,5-DMC from the perspective of molecular adsorption modeling. Thus, the value of 1,8-/2,5-DMC would be increasing along the oil filling pathway. This is consistent with our measured values from subsurfaces, which implies that dimethyl carbazole compounds are effective as migration indicators.[59]

3.7. Application of Tracing Results in Hydrocarbon Exploration. The hydrocarbons migrated along certain preferable pathway subsurfaces. Large-scale faults, structural fractures, and lithology changes could affect the migration pathway.[13,59] Figure 11 shows the SE−NW cross section across the study area. The figure shows the fault system connecting the wells Hu41, Hu82, Hu40, Hu39-12, Hu39-20, and Hu7 and the inferred oil filling pathway. The four pyrrolic parameters (1,8-/2,7-DMC, 1,8-/2,5-DMC, 1,8-/N-exposed DMC, and G1 N-shielded %) increase the updip gradually (Figure 7). It can be predicted that the overall trend could be that the oil migrates vertically from the Haitongji Sag along the Changyuan Fault to the fault block where Hu39-20 is located at the structural high. In specific, the oil migrated vertically from the Haitongji Sag along the Changyuan Fault to the beds of the hanging wall through the Well Hu82 (supported by the pyrrolic data from the oil sands sampled) and then migrated laterally in the carrier beds. Based on the varying trend of the four pyrrolic parameters, it could be inferred that the lateral migration direction is from SE to NW. On encountering Well Hu39-12, they continue to migrate vertically upward along the fault where Hu39-12 is

https://doi.org/10.1021/acsomega.2c00003
ACS Omega 2022, 7, 8103−8114

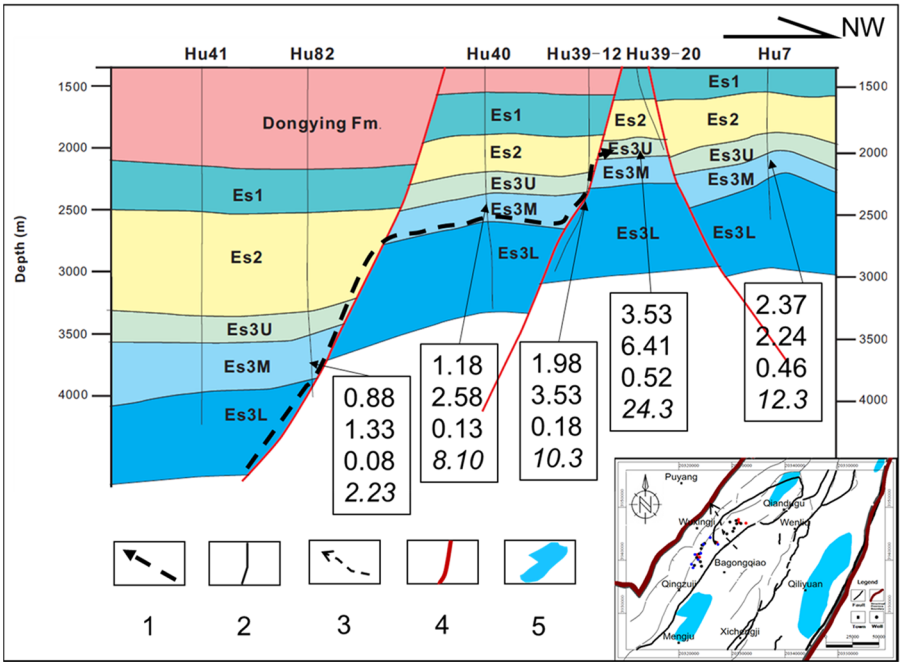

Figure 11. SE−NW cross-section connection wells Hu41, Hu82, Hu40, Hu39-12, Hu39-20, and Hu7 showing the fault systems and oil migration routes. The values from top to bottom represent the following parameters: 1.8-/2,7-DMC, 1.8-/2,5-DMC, 1.8-/N-exposed-DMC, and G1 N-shielded DMC %, respectively. Legend: (1) oil migration orientation; (2) well trajectory; (3) location of cross section; (4) fault; and (5) hypothetical boundary of the Haitongji Sag.

penetrated through, and then migrate laterally further to the fault block where Hu39-20 is located at the structural high. The above speculations are consistent with the previous studies on the Changyuan Fault. The Changyuan Fault has been assumed to be the major pathway of vertical migration in this area due to its large fault displacement and cutting through multiple reservoir strata. The Changyuan Fault enables oil to migrate and accumulate in the reservoir beds of the hanging wall along the fault plane, with the Haitongji Sag in the proximity of the footwall as the oil source,[60−64] which could be confirmed by the varying trend of the pyrrolic parameters in this study. In general, the smaller the parameter value the shorter the migration distance and the closer the oil source. Zones in the Western Slope Belt situated upstream of the preferred oil filling pathways, are likely to be the most favorable prospecting regions. In addition, the discovered reserves are much lower than those estimated on the basis of mass balance calculation.[39] Therefore, it is reasonable to upgrade the blocks, like B-15 situated in the proximity of the Haitongji Sag as the oil source, where hydrocarbons migrated a short distance and could be "sealed" by faults as a promising area to explore in the future.

4. CONCLUSIONS

A set of crude oils and oil-bearing sand extracts from the Eocene syn-rift fault-blocked clastic reservoirs in the Huzhuangji area (Western Slope Belt) of Dongpu Depression, Bohai Bay Basin (East China), were geochemically analyzed. All of the oils and oil-bearing sand extracts show significant similarities in biomarker signatures, indicating that all of the oils were derived from the same source kitchen. They belong to the same oil family, showing no obvious biodegradation, and are at approximately the same maturity level. Thus, the variations in carbazoles in oils from the same source rock/kitchen are mainly controlled by the relative migration fractionation effect. In the middle Es3 contour map with carbazole isomer ratios tracing the oil filling pathways, the direction of increase of these parameters (1,8-/2,7-DMC ratio, 1,8-/2,5-DMC ratio, 1,8-/N-exposed DMC ratio, and G1 N-shielded DMC %) indicates the preferential oil migration direction and filling pathways. These results show that parameters relating to dimethyl carbazoles can be used as molecular tracers for filling orientation and pathways in lacustrine syn-rift fault-blocked sandstone reservoirs.

5. SAMPLES AND METHODS

5.1. Study Area and Sampling. Samples were taken from the relevant wells in the Huzhuangji area (western slope belt) of Dongpu Depression (Figure 1), including 31 crude oils and 2 oil-bearing sand extracts. Gas chromatography (GC) and gas chromatography−mass spectrometry (GC−MS) analyses of the samples were carried out in the Key Laboratory of Exploration Technologies for Oil and Gas Resources (Yangtze University, Wuhan, China).

5.2. Isolation of Organic Nitrogen Compounds. All of the oil samples were deasphaltened using 60 mL of *n*-hexane. Then, the samples were fractionated by liquid chromatography on a Pasteur pipette using silica gel/alumina columns (1:1, w/w; 60−100 mesh) into saturated and aromatic hydrocarbon fractions with 5 mL of *n*-hexane and 6 mL of a mixture of hexane and dichloromethane (7:3, v/v) as eluents, respectively. NSO and some of the polyaromatic compounds were obtained by elution with 5 mL of dichloromethane and methanol (95:5, v/v).

The method used for the isolation of polar compounds was modified from that developed by Later et al.[45] Briefly, for each sample, 0.5−1.0 mg of the NSO fraction was dissolved in hexane and adsorbed onto 0.5 g of silicic acid hydrate powder, and the solvent was removed by stirring the mixture under nitrogen gas. A 22 cm column was packed with 2 g of silicic acid powder in the form of a slurry with hexane. After introducing the 0.5 g silicic acid powder with the adsorbed NSOs on top, the following

https://doi.org/10.1021/acsomega.2c00003
ACS Omega 2022, 7, 8103−8114

fractions were eluted: low-polar compounds (LPCs) with 50 mL of a mixture of 85:15 (v/v) hexane/DCM and high-polar compounds (HPCs) with 50 mL of a mixture of 95:5 (v/v) DCM/methanol. Carbazole, benzocarbazole, and their derivatives eluted with the low-polar NSO fraction. The low-polar NSO fraction was diluted with DCM to a concentration of 3 mg/mL for further analysis by GC−MS. The high-polar fractions were collected and weighed.

5.3. Gas Chromatography. The isolated fractions, saturates, and aromatics were analyzed, respectively, using an Agilent 6890 series GC with a splitless capillary injector and a 30 m × 0.25 mm (i.d.) J&W Scientific DB-5 122-5032 fused silica capillary column coated with a 0.25 μm liquid film. The injector was set up in the splitless injection mode, and the temperature was held at 300 °C. The carrier gas was helium (He) with a flow rate of 1.4 mL/min. The temperature program was started with an initial temperature of 40 °C, held for 1.5 min, and increased to 300 °C at the rate of 4 °C per minute followed by an isothermal period of 34 min for a total run time of 100.5 min. The flame ionization detector (FID) temperature was set at 310 °C. *n*-Alkanes and isoprenoids were identified in each chromatogram by comparing their relative retention time with standards.

5.4. Gas Chromatography−Mass Spectrometry. The GC−MS analyses were carried out with an Agilent Technologies 7890A gas chromatograph coupled with an Agilent Technologies 5975C mass spectrometer. For the biomarker analysis, selected ions were chosen to analyze samples in the single-ion monitoring (SIM) or multiple-ion detection (MID) mode. The ion source operated in the electron impact mode with an energy of 70 eV.

The GC was equipped with a 60 m × 0.32 mm (i.d.) J&W Scientific DB-5MS fused silica capillary column coated with a 0.25 μm liquid film. For the saturated and aromatic compound analysis, the ion source temperature was 200 °C, injector temperature was 300 °C, and transfer line temperature was 310 °C. The GC temperature program was started at 40 °C, held for 1.5 min, increased to 300 °C at the rate of 4 °C per minute, and then held at 300 °C for 34 min for a total run time of 100.5 min. For the low-polar fraction nitrogen compounds, the temperature program was started at 40 °C with a 1.5 min hold time and was later increased to 300 °C at the rate of 4 °C per minute and then held isothermal for 25 min for a total run time of 90.5 min.

AUTHOR INFORMATION

Corresponding Author

Ting Wang − *Hubei Key Laboratory of Petroleum Geochemistry and Environment, Yangtze University, Wuhan 430100, China; State Key Laboratory of Organic Geochemistry, Guangzhou 510640, China;* orcid.org/0000-0001-7643-5666; Email: tw@yangtzeu.edu.cn

Authors

Youjun Tang − *Hubei Key Laboratory of Petroleum Geochemistry and Environment, Yangtze University, Wuhan 430100, China*

Ruilin Wang − *Hubei Key Laboratory of Petroleum Geochemistry and Environment, Yangtze University, Wuhan 430100, China*

Donglin Zhang − *Hubei Key Laboratory of Petroleum Geochemistry and Environment, Yangtze University, Wuhan 430100, China*

Xiaoqiang Liu − *State Key Laboratory of Petroleum Resources and Prospecting, College of Geosciences, China University of Petroleum, Beijing 102249, China; College of Chemistry and Environmental Engineering, Sichuan University of Science and Engineering, Zigong 643000, China*

Hongbo Li − *Hubei Key Laboratory of Petroleum Geochemistry and Environment, Yangtze University, Wuhan 430100, China*

Tianwu Xu − *Sinopec Zhongyuan Oilfield, Puyang, Henan 457001, China*

Yunxian Zhang − *Sinopec Zhongyuan Oilfield, Puyang, Henan 457001, China*

Chengfu Zhang − *Sinopec Zhongyuan Oilfield, Puyang, Henan 457001, China*

Yahao Huang − *Hubei Key Laboratory of Petroleum Geochemistry and Environment, Yangtze University, Wuhan 430100, China*

Complete contact information is available at: https://pubs.acs.org/10.1021/acsomega.2c00003

Author Contributions

#Y.T. is the first author.

Funding

The authors would like to express their thanks to the Open Foundation of the State Key Laboratory of Organic Geochemistry (SKLOG202019), National Natural Science Foundation of China (No. 41972148), National Natural Science Foundation of China (No. 41802152), and Open Foundation of Top Disciplines in Yangtze University (No. 2019KFJJ0818016) for providing financial support.

Notes

The authors declare no competing financial interest.

ACKNOWLEDGMENTS

The authors are grateful to Cuishan Zhu for assistance with the GC−MS analysis. The authors would like to recognize the Sinopec Zhongyuan Oilfield for their generous donation of samples and additional information.

REFERENCES

(1) Jiang, Y. L.; Zahng, Y. Main geological factors controlling the accumulation and distribution of oil and gas in a complicated fault-block region. *Pet. Explor. Dev.* **1999**, *5*, 39−42.

(2) Li, Y.; Gao, X.; Meng, S.; Wu, P.; Niu, X. L.; Qiao, P.; Elsworth, D. Diagenetic sequences of continuously deposited tight sandstones in various environments: A case study from upper Paleozoic sandstones in the Linxing area, eastern Ordos basin, China. *AAPG Bull.* **2019**, *103*, 2757−2783.

(3) Li, Y.; Yang, J.; Pan, Z.; Meng, S. Z.; Wang, K.; Niu, X. L. Unconventional natural gas accumulations in stacked deposits: a discussion of Upper Paleozoic coal-bearing strata in the east margin of the Ordos Basin, China. *Acta Geol. Sin.* **2019**, *93*, 111−129.

(4) Li, Y.; Zw, A.; Peng, W. C.; Gao, X. D.; Yu, Z. L.; Yu, Y.; Yang, J. H. Organic Geochem of Upper Paleozoic source rocks in the eastern margin of the Ordos Basin, China: Input and hydrocarbon generation potential. *J. Pet. Sci. Eng.* **2019**, *181*, No. 106202.

(5) Karim, A.; Piper, P. G.; Piper, D.J.M. Controls on diagenesis of Lower Cretaceous reservoir sandstones in the western Sable Subbasin, offshore Nova Scotia. *Sediment. Geol.* **2010**, *224*, 65−83.

(6) Lai, J.; Wang, G. W.; Chai, Y.; Xin, Y.; Wu, Q. K.; Zhang, X. T.; Sun, Y. H. Deep burial diagenesis and reservoir quality evolution of high-temperature, high-pressure sandstones: Examples from Lower Cretaceous Bashijiqike Formation in Keshen area, Kuqa depression, Tarim basin of China. *AAPG Bull.* **2017**, *101*, 829−862.

(7) Nygaard Hansen, H.; Løvstad, K.; Müller, R.; Jahren, J. Clay coating preserving high porosities in deeply buried intervals of the Stø Formation. *Mar. Pet. Geol.* **2017**, *88*, 648−658.

(8) Taylor, T. R.; Giles, M. R.; Hathon, L. A.; Diggs, T. N.; Braunsdorf, N. R.; Birbiglia, G. V.; et al. Sandstone diagenesis and reservoir quality prediction: models, myths, and reality. *AAPG Bull.* **2010**, *94*, 1093−1132.
(9) England, W. A.; Mackenzie, A. S.; Mann, D. M.; Quigley, T. M. The movement and entrapment of petroleum fluids in the subsurface. *J. Geol. Soc.* **1987**, *144*, 327−347.
(10) Larter, S. R.; Bowler, B. F. J.; Li, M.; Chen, M.; Brincat, D.; Bennett, B.; Noke, K.; Donohoe, P.; Simmons, D.; Kohnen, M.; et al. Molecular indicators of secondary oil migration distances. *Nature* **1996**, *383*, 593−597.
(11) Li, M.; Larter, S. R.; Stoddart, D.; Bjoroy, M. Fractionation of pyrrolic nitrogen compounds in petroleum during migration: derivation of migration-related geochemical parameters. *Geol. Soc. London, Spec. Publ.* **1995**, *86*, 103−123.
(12) Li, M.; Fowler, M. G.; Obermajer, M.; Stasiuk, L. D.; Snowdon, L. R. Geochemical characterisation of Middle Devonian oils in NW Alberta, Canada: possible source and maturity effect on pyrrolic nitrogen compounds. *Org. Geochem.* **1999**, *30*, 1039−1057.
(13) Dorbon, M.; Schmitter, J. M.; Arpino, A.; Guiochon, G. Carbozoles et lactames du petrole methode d'extraction et caraterisation. *J. Chromatogr.* **1982**, *246*, 255−269.
(14) Dorbon, M.; Schmitter, J. M.; Garrigues, P.; Ioannis, I.; Ewald, M.; Patrick Arpino, G.; Guiochon, G. Distribution of carbazole derivatives in petroleum. *Org. Geochem.* **1984**, *7*, 111−120.
(15) Ignatiadis, I.; Schmitter, J. M.; Dorbon, M.; Toulhoat, H.; Arpino, P. *Influence des hydrotraitments catalytiques sur la distrubution des composés azotés d'un gas-oil, de coking et d'une huile lourde désasphaltee. Characterization of Heavy Crude Oils and Petroleum Residues*; Technip Paris, 1984; Vol. *423*, pp 89−97.
(16) Bakel, A. J.; Philp, R. P. The distribution and quantitation of organonitrogen compounds in crude oils and rock pyrolysates. *Org. Geochem.* **1990**, *16*, 353−367.
(17) Yamamoto, M. Fractionation of azarenes during oil migration. *Org. Geochem.* **1992**, *19*, 389−402.
(18) Li, M.; Larter, S. R.; Stoddart, D.; Bjorøy, M. Liquid chromatographic separation schemes for pyrrole and pyridine nitrogen aromatic heterocycle fractions from crude oils suitable for rapid characterization of geochemical samples. *Anal. Chem.* **1992**, *64*, 1337−1344.
(19) Harrison, E.; Telnaes, N.; Wilhelms, A.; Horsfield, B.; Van Duin, A.; Bennett, B.; Larter, S. In *Maturity Controls on Carbazole Distributions in Coals and Source Rocks*, 18th International Meeting on Organic Geochemistry; IEEE, 1997; pp 235−236.
(20) Clegg, H.; Wilkes, H.; Oldenburg, T.; Santamaría-orozco, D.; Horsfield, B. Influence of maturity on carbazole and benzocarbazole distributions in crude oils and source rocks from the Sonda de Campeche, Gulf of Mexico. *Org. Geochem.* **1998**, *29*, 183−194.
(21) Hwang, R. J.; Heidrick, T.; Mertani, B.; Li, M.; et al. Correlation and migration studies of North Central Sumatra oils. *Org. Geochem.* **2002**, *33*, 1361−1379.
(22) Hallmann, C. O.; Arouri, K. R.; McKirdy, D. M.; Schwark, L. Temporal resolution of an oil charging history−a case study of residual oil benzocarbazoles from the Gidgealpa Field. *Org. Geochem.* **2007**, *38*, 1516−1536.
(23) Huang, H.; Bowler, B. F. J.; Zhang, Z.; Oldenburg, T. B. P.; Larter, S. R. Influence of biodegradation on carbazole and benzocarbazole distributions in oil columns from the Liaohe basin, NE China. *Org. Geochem.* **2003**, *34*, 951−969.
(24) Clegg, H.; Wilkes, H.; Horsfield, B. Carbazole distributions in carbonate and clastic source rocks. *Geochim. Cosmochim. Acta* **1997**, *61*, 5335−5345.
(25) Zhu, Q.; Money, S. L.; Russell, A. E.; et al. Determination of the fate of nitrogen functionality in carbonaceous materials during pyrolysis and combustion using X-ray absorption near edge structure spectroscopy. *Langmuir* **1997**, *13*, 2149−2157.
(26) Bakr, M. M. Y.; Wilkes, H. The influence of facies and depositional environment on the occurrence and distribution of carbazoles and benzocarbazoles in crude oils: a case study from the Gulf of Suez, Egypt. *Org. Geochem.* **2002**, *33*, 561−580.
(27) Bennett, B.; Olsen, S. D. The influence of source depositional conditions on the hydrocarbon and nitrogen compounds in petroleum from central Montana, USA. *Org. Geochem.* **2007**, *38*, 935−956.
(28) Zhang, C.; Zhang, Y.; Zhang, M.; Zhao, H.; Cai, C. Carbazole distributions in rocks from non-marine depositional environments. *Org. Geochem.* **2008**, *39*, 868−878.
(29) Wang, T. G.; Li, S. M.; Zhang, S. C. Oil migration in the Lunnan region, Tarim Basin, China based on the pyrrolic nitrogen compound distribution. *J. Pet. Sci. Eng.* **2004**, *41*, 123−134.
(30) Sivan, P.; Datta, G. C.; Singh, R. R. Aromatic biomarkers as indicators of source, depositional environment, maturity and secondary migration in the oils of Cambay Basin, India. *Org. Geochem.* **2008**, *39*, 1620−1630.
(31) Duan, Y.; Yuan, Y.; Qian, R. Migration features of crude oil in fluvial deposits of Maling oilfield in Ordos Basin, China. *Org. Geochem.* **2013**, *58*, 78−85.
(32) Wang, P. X.; Wang, X. J. *Reservoir Potential of Huqing Area in Western Slope of Dongpu Depression*; Inner Mongolia Petrochemical Industry, 2012; Vol. *38*, pp 136−138.
(33) Chen, X. F. *Hydrocarbon Generation and Accumulation Effect of Saline Lacustrine Strata Bearing Gypsum-Salt Rock in Dongpu Sag, Bohai Bay Basin*; China University of Petroleum: Beijing, 2017.
(34) Han, X. Q.; Wang, L. Z.; He, F. Hydrocarbon Accumulation Conditions and Potential Analysis of Hu-Qing Fault Step Zone in Dongpu Depression. *Pet. Geol. Eng.* **2003**, *17*, 10−12.
(35) Wu, X. H.; Lv, X. H. The Geochemistry Character of Hydrocarbon Source Rocks of Huqing Oil Field in Dongpu Sag. *Offshore Oil* **2005**, *25*, 29−35.
(36) Liu, Z. W.; Yang, G. F.; Wang, Y. Deep zone reservoir-forming condition in the first step of Hu-qing oilfield in the Dongpu sag. *J. Lanzhou Univ.* **2006**, *42*, 7−10.
(37) Hao, J. G.; Jiang, Y. L.; Liu, J. D. Accumulation period and accumulation process of hydrocarbon in Huqing Area of Dongpu Depression. *Fault-Block Oil Gas Field* **2013**, *20*, 38−42.
(38) Zhang, Y. X.; Shen, Z. M.; Liu, H. Y. Characteristics of the reservoir geochemistry of the west slope in the Dongpu Depression, Henan, China. *J. Chengdu Univ. Technol.* **2007**, *34*, 531−537.
(39) Zhang, D. L.; Tang, Y. J.; Li, H. B.; Xu, T. W.; Zhang, Y. X.; Zhang, C. F.; Huang, Y. H.; Wang, T. Methyltrimethyltridecylchromans in Mature Oils from Saline Lacustrine Settings in the Dongpu Depression, Bohai Bay Basin, East China. *ACS Omega* **2021**, *6*, 17400−17412.
(40) Tang, W. X. Hydrocarbon accumulation dynamics of Huqing fault zone in Dongpu depression. *J. China Univ. Geosci.* **2008**, 65−66.
(41) Li, L.; Li, S.; Zhang, H. A.; Xu, T. W. Characteristics and Formation Mechanisms for the Saline Lacustrine Oil in the West Slope of the Dongpu Sag. *Mar. Pet. Geol.* **2018**, *32*, 1109−1124.
(42) Ji, H.; Li, S.; Greenwood, P.; Zhang, H.; Pang, X.; Xu, T.; He, N.; Shi, Q. Geochemical characteristics and significance of heteroatom compounds in lacustrine oils of the Dongpu Depression (Bohai Bay Basin, China) by negative-ion Fourier transform ion cyclotron resonance mass spectrometry. *Mar. Pet. Geol.* **2018**, *97*, 568−591.
(43) Li, S.; Pang, X.; Zhang, H. In *Origin of "Immature" Saline Lacustrine Oils in the Dongpu Depression, Bohai Bay Basin*, 29th International Meeting on Organic Geochemistry; European Association of Geoscientists & Engineers, 2019.
(44) Gao, H. C. Sequence stratigraphy of paleogene shahejie formation in dongpu depression, bohai bay basin. *Pet. Nat. Gas Geol.* **2011**, *32*, 839−850.
(45) Dong, Y. X. Characteristics of braided river delta deposition and deep reservoir in bohai bay basin—a case study of the first member of paleogene sand in the southern part of nanpu depression. *Pet. Explor. Dev.* **2014**, *41*, 385−392.
(46) Liu, L.; Ren, Z. Thermal evolution of Dongpu sag. *Pet. Explor. Dev.* **2007**, *34*, 419−418.

https://doi.org/10.1021/acsomega.2c00003
ACS Omega 2022, 7, 8103−8114

(47) Ji, Y.; Zhou, S.; Cheng, T. Application of sequence stratigraphy to subtle oil−gas reservoir exploration: take example of the third member Shahejie formation Dongpu Depression. *Acta Geol. Sin.* **2015**, *89*, 395.
(48) Li, X.; Zhang, J.; Xie, J. Sedimentary and sequence-stratigraphic characteristics of the lower second submember, Shahejie formation, M1 block, Wenmingzhai oilfield, Dongpu depression, China. *Arab. J. Geosci.* **2015**, *8*, 5397−5406.
(49) Man, H. Y.; Ye, J. L.; Li, L. X.; Xu, J. J.; Wang, J. L. Characteristics of Oilfield Water and Its Implications to Petroleum Geology in the Western Slope Belt, Dongpu Depression. *Geol. Sci. Technol. Inf.* **2009**, *28*, 67−72.
(50) Later, D. W.; Lee, M. L.; Bartle, K. D.; Kong, R. C.; Vassilaros, D. L. Chemical class separation and characterization of organic compounds in synthetic fuels. *Anal. Chem.* **1981**, *53*, 1612−1620.
(51) Wang, T. G.; Zhong, N. N.; Hou, D. J.; Bao, J. P.; Huang, G. H.; Li, X. Q. Several Genetic Mechanisms of Immature Crude Oils in China. *Acta Sedimentol. Sin.* **1997**, *2*, 75−83.
(52) Moldowan, J. M.; Fago, F. J.; Lee, C. Y. Relationship between petroleum composition and depositional environment of petroleum source rocks. *AAPG Bull.* **1985**, *69*, 1225−1268.
(53) Philp, R. P.; Jones, P. J.; Lin, L. H. An organic geochemical study of oils, source rocks, and tar sands in the Ardmore and Anadarko basins. *Circ. - Okla. Geol. Surv.* **1989**, *90*, 65−76.
(54) Moldowan, J. M.; Lee, C. Y.; Sundararaman, P. Source correlation and maturity assessment of selected oils and rocks from the Central Adriatic Basin (Italy and Yugoslavia). *Am. Chem. Soc. Div. Pet. Chem. Prepr.* **1992**, 370−401.
(55) Deng, Y. N.; Wang, Y.; Chen, H. D. Bivalves and gastropods from the Ordovician Guanyinqiao Member of the Wufeng Formation in Tongzi, Guizhou, South China, and their ecological significance. *J. Stratigr.* **2010**, *34*, 328−333.
(56) Wang, T. G.; Li, S. M.; Zhang, A. Y.; Zhu, L.; Li, B. H.; Zhou, Y. B. Oil migration analysis with pyrrolic nitrogen compounds. *J. Univ. Pet., China* **2000**, *24*, 83−86.
(57) He, G. Y.; Guan, P.; Tan, Y. H.; Li, Y. K.; Zhang, W. T.; Du, B. B.; Yu, H. J. The path of hydrocarbon charge and accumulation in Nanyishan oilfield of the northwest Qaidam Basin. *Acta Sedimentol. Sin.* **2009**, *27*, 769−776.
(58) Li, S. M.; Pang, X. Q.; Li, M. W.; Jin, Z. J. Characteristics of pyrrolic nitrogen compounds and their geochemical significance in oils and rocks of Bamianhe oilfield, eastern China. *Geochemica* **2002**, *31*, 1−7.
(59) Han, Q.; Li, M.; Liu, X.; et al. Fractionation of alkylated carbazoles in petroleum during subsurface migration: Evidence from molecular simulation and application in sandstone reservoirs. *J. Pet. Sci. Eng.* **2020**, *191*, No. 107308.
(60) Hindle, A. D. Petroleum migrati on pathways and charge concentration: a three-dimensional model. *AAPG Bull.* **1997**, *81*, 1451−1481.
(61) Li, B. L.; Wang, M. M.; Wei, G. Q. Lateral migration and accumulation of biogenic gas in the Sanhu Area, Qaidan Basin. *Geol. Rev.* **2003**, *49*, 93−100.
(62) Wang, Z. L.; Ma, W. M.; Xiang, R. Z.; Zhnag, J. B.; Ceng, T.; Mu, X. S. Law and model of reservoir-formation about complex fault-block in Dongpu Depression. *Fault-Block Oil Gas Field* **2002**, *9*, 15−18.
(63) He, F.; Yang, Y. L.; Lv, Y. H.; Li, J. R. Analysis of Hydrocarbon Exploration Potential in the West Slope Zone of Dongpu Depression. *J. Oil Gas Technol.* **2004**, *26*, 25−26.
(64) Li, Y.; Lv, X. H.; Zhou, Y. J. Analysis of hydrocarbon accumulation conditions and exploration potential in the complex fault block zone on the Western Slope of Dongpu Depression. *J. Oil Gas Technol.* **2005**, *27*, 166−170.

https://doi.org/10.1021/acsomega.2c00003
ACS Omega 2022, 7, 8103−8114